ARTICLE IN PRESS

Journal of Rock Mechanics and Geotechnical Engineering xxx (xxxx) xxx

Contents lists available at ScienceDirect

Journal of Rock Mechanics and Geotechnical Engineering

journal homepage: www.rockgeotech.org

Design adaptations in a large and deep urban excavation: Case study

Amir Alipour, Abolfazl Eslami*

Department of Civil and Environmental Engineering, Amirkabir University of Technology, Tehran, Iran

ARTICLE INFO

Article history:
Received 28 June 2018
Received in revised form
19 August 2018
Accepted 31 August 2018
Available online xxx

Keywords:
Deep excavation
Field observations
In situ tests
Support system
Adaptive design
Inverse analysis

ABSTRACT

In this paper, design, re-design, and performance of a long-standing very deep excavation, which was originally planned to depth of 38 m, are presented. Over-digging was not planned in the original design, thus the reassessment was performed. Two main topics were followed: deepening to increase the maximum depth of an existent excavation from 38 m to 42.5 m, and feasibility for upgrading a predesigned support system from temporary to permanent support system. The geological investigations in the project site illustrated a type of stiff and cemented coarse-grained alluvium. An observational approach with additional geotechnical investigations and in situ tests was applied. Back analyses of stability of an unsupported access ramp, as well as deformation monitoring of walls, were used in order to review geotechnical design parameters that represent the full-scale behavior of the ground. Additional nails and soldier piles together with building mat foundation were implemented as a complementary lateral support in the retaining system. From an engineering point of view, by assuming a corrosion rate of 0.065 mm/a for existent rebars, according to chemical and electrical resistivity tests, the long-term performance of the revised retaining system was verified by static and pseudo-dynamic ultimate limit state analyses. Performance monitoring during the construction shows that the measured deformation is in the lower limit of the prediction.

1. Introduction

Due to the rapid population growth in urban areas, deep and large underground excavations have been increased in the world. In many countries such as China (Tan and Wang, 2013), Turkey (Durgunoglu et al., 2007; Durgunoglu, 2008), Portugal (Pinto et al., 2007), and France (Gastebled and Baghery, 2010), there are case studies of very deep and large excavations that have been reported.

The performance of earth structures such as excavation is extremely complex, since their real behaviors often differ from the ones predicted at the initial design stages. This inconsistency is due to the fact that many uncertainties are involved in both geological and geomechanical characteristics of soil masses, as well as in the initial stresses acting in them. To fill in the gap between the measured and predicted behaviors, Terzaghi and Peck (1948) proposed an observational procedure, which is an integrated design-construction method for the earth structures. According to the method, the performance of the structures is monitored by the field measurements, usually displacement measurement during constructions. In addition, the validity of the original design can be verified, and if necessary, the original design can be modified. Peck (1969) formally introduced the observational method (OM) in a specific paper. Some of the applications of OM has been reported through the geotechnical projects (e.g. Glass and Powderham, 1994; Powderham, 1994, 2002; Powderham and Rutty, 1994; Peck, 2001; Sakurai et al., 2003; Chapman and Green, 2004; Finno and Calvello, 2005; Yeow and Feltham, 2008; Yeow et al., 2014; Spross and Johansson, 2017; Fuentes et al., 2018).

Numerical simulations are extensively used in the development, design, and analysis of excavation problems to represent the behavior of system. The use of such a model-based simulation in engineering practice often necessitates estimating model parameters based on field measurements. This kind of problems is often referred to as inverse problems or back analysis. The adoption of back analysis by the geotechnical community began in the early 1980s. Gioda (1980) and Gioda and Maier (1980) presented one of the first geotechnical back analyses, where the identification of rock mass parameters during a tunnel excavation was carried out. The least squares criterion was used to define the objective function, while a direct method was adopted to minimize it. Inverse analysis techniques may be very helpful in such an effort, as model

* Corresponding author.
E-mail address: afeslami@aut.ac.ir (A. Eslami).

Peer review under responsibility of Institute of Rock and Soil Mechanics, Chinese Academy of Sciences.

https://doi.org/10.1016/j.jrmge.2018.08.014
1674-7755

Fig. 1. A very deep excavation in the northern part of Tehran with the maximum depth of 70 m.

calibration is performed by iteratively changing the estimates of its input parameters until the value of an objective function, which quantifies the errors between observed data and computed results, is minimized. When this occurs, an "observational modeling" approach is in fact employed (Calvello, 2017).

Ikuta et al. (1994) proposed an OM whereby the excavation sequence was modified and optimized during construction. They concluded that the method could be used to revise and confirm the design assumptions by inverse analysis of initial excavation stages. New design assumptions were implemented to predict the behavior of the subsequent stages. Following the trend initiated by Gioda (1980), the Japanese group (formed by the universities of Kobe, Kyoto and Tokyo) was strongly working on the field of back analysis applied to geotechnics. Several back analyses were conducted by Sakurai (1983), Sakurai and Takeuchi (1983) and Hisatake and Ito (1985) for tunnel excavations, as well as Arai et al. (1984) for consolidation and Arai et al. (1986) for testing embankments on soft clay deposits. Later, Ledesma (1987) introduced a full definition of the back analysis problem based on the concept of maximum likelihood to generalize the objective function and formally define it from a statistical point of view. Moreover, he defined the structure of the error for several well-known in situ instruments such as inclinometers and sliding micrometers. Using the methodology presented in Ledesma (1987), several real cases studies of tunnels and excavation were carried out in Gens et al. (1988, 1996), Ledesma et al. (1996) and Ledesma and Romero (1997). Application of in situ full-scale tests to design of anchored sheet-piled retaining wall was illustrated by Young and Ho (1994). In this study, an instrumented trial installation of a short panel of sheet piling was made to assess the movements induced by excavation, pile installation, and extraction. This trial was back-analyzed using the CRISP finite element program, and the results were used to predict the movements of the full-scale structure. Instrumentation was installed on the sheet piles and power cables to monitor the movements and adjust the construction procedure in the event of unacceptably high movements recorded. In Finno and Calvello (2005), the inverse analysis of a real supported excavation performed in five stages was presented. The field observations were obtained from inclinometer data and the hardening soil (HS) model was used as the constitutive model to reproduce the soil behavior. The results indicated that a recalibration of the model at an early construction stage might affect the predictions throughout construction. Zhang et al. (2015, 2017, 2018) studied parameter estimation, updating predictions, and adaptive design of braced excavations.

However, it is a matter of great concern, especially in practical applications to investigate design adjustments during or after the construction of existing deep and large excavations due to nearby construction in urban areas. Furthermore, implementation of observations for over-digging feasibility of long-standing existent deep excavations has not been reported. Therefore, in this paper, the short- and long-term performances of a long-standing deep urban excavation were investigated, where deepening for the construction of additional basement floors as well as nearby excavation effects was the main issue. With an adaptive design approach, it is found that re-evaluation of an earth retaining support system remarkably leads to an economical design.

2. Project description

With a population of about 15 million in its larger metropolitan area, Tehran has one of the largest metropolitan areas in the Middle East. The average depth of excavations in Tehran ranges from 20 m to 40 m. In some situations, depths up to 50 m and 70 m have been reported. Fig. 1 illustrates a very deep soil nailing and anchoring supported excavation in the northern part of Tehran with a maximum height of about 70 m.

Tehran is located at the bottom of the southern slopes of the Alborz Mountains Range and lies on an alluvial plain formed over time by flood erosion of the mountains. Due to this process, large and small particles have settled on high and low elevations, respectively, resulting in varying geological conditions (Fakher et al., 2007). The northern part of the city is at a higher elevation than the southern part. Therefore, the surface and underground water flows from the north to the south. The groundwater is not a serious problem in excavation projects in Tehran. Due to a deep groundwater table, excavation works are usually performed using soil nailing or anchoring systems without a pre-constructed diaphragm or sheet pile embedded wall. Thus, a bottom-up basement construction method is the common practice. Local water sources such as sewers, pipe leakages, and natural groundwater flows are usually the main causes for implementing a draining system in excavation works. These locally held groundwater regimes and underground streams could usually be pumped out of the site during construction.

A deep excavation for construction of a multi-purpose twin tower that has 25 floors above the ground surface and 6-storey underground basement was studied in this paper. The area of the project was about 14,308 m^2. Due to a sloped natural ground

Please cite this article as: Alipour A, Eslami A, Design adaptations in a large and deep urban excavation: Case study, Journal of Rock Mechanics and Geotechnical Engineering, https://doi.org/10.1016/j.jrmge.2018.08.014

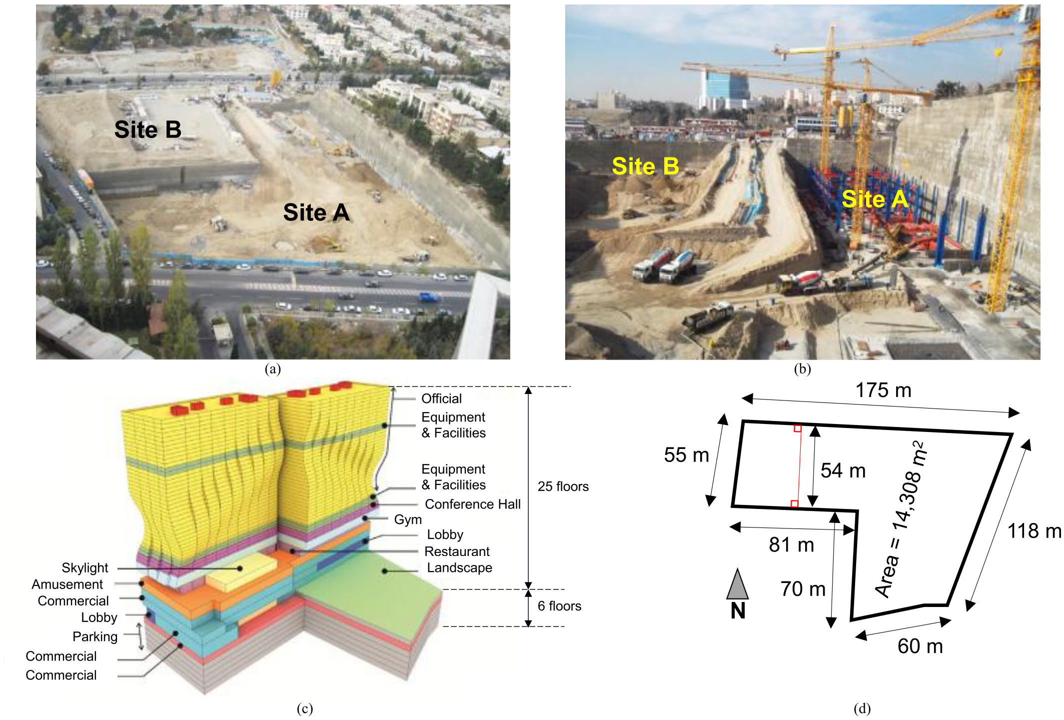

Fig. 2. An overview of sites A and B in (a) the initial and (b) final stages; (c) multi-purpose twin tower (main building of the project); and (d) geometry of site A.

surface, the excavation depth was not constant throughout the site. A differential elevation of about 10 m existed from the north to the south before construction. In the original design, the maximum depth of excavation was 38 m in the northern side.

The original design of the retaining system was based on a temporary soil nailing with 15 cm shotcrete facing. The over-digging was not planned in the original design, thus the reassessment must be investigated. Another issue, because of nearby excavation, was upgrading the temporarily existing retaining system to a permanent one. This was caused by the fact that the nearby under-construction building had an excavation 6 m deeper than the project under study. Therefore, removing soil pressures from one side of the main building's basement would have led to an unbalanced force, which was not considered in the original design. The building could not support this unbalanced earth pressure. Calculations according to the Iranian earthquake building code (BHRC, 2007) showed that the unbalanced force induced by the removal of 42.5 m soil imposes a remarkable base shear force similar to a large earthquake (with the peak ground acceleration (PGA) of 0.35 g) on the building as a permanent dead load. The unbalanced earth load and the earthquake shear load are respectively calculated as follows:

$$V_{\mathrm{Earth}} = 0.5\gamma K_{\mathrm{a}} h^2 = 0.5 \times 20 \times 0.22 \times 42.5^2 = 3928 \text{ kN/m} \quad (1)$$

$$\begin{aligned} V_{\mathrm{Earthquake}} &= CW = CnwB = 0.21 \times 31 \times 12 \times 53 \\ &= 4140 \text{ kN/m} \end{aligned} \quad (2)$$

where V_{Earth} is the total shear force produced by the unbalanced earth pressure; γ is the unit weight of soil; K_{a} is the active earth pressure coefficient by giving the effective internal friction angle $\phi' = 40°$; h is the excavation depth; $V_{\mathrm{Earthquake}}$ is the total shear force produced by the earthquake; C is a coefficient related to the PGA, building response, and building design categories; n is the number of floors; w is the floor load; and B is the building width.

From an engineering point of view, there is a preference to upgrade the existing temporary retaining system to the permanent one if technically feasible.

Fig. 2 presents an overview of sites A (studied in this paper) and B (nearby construction). It illustrates the construction of site A during the initial stage when the project in site B was not commenced. In the same manner, it displays the final stages of construction when the project in site A is in the structural phase while the project in site B is in the middle of excavation works. Site A has an L-shaped geometry in the plan. The excavation works took about 3 years. During the construction period, the operations had been ceased occasionally due to non-technical issues.

3. Geotechnical conditions

The project site was located in the northern part of Tehran with a special type of soil formation. Local geologists and engineers use Rieben's (1966) classification of Tehran alluvium. He divided the Tehran coarse-grained alluvium into four categories, ranging from the oldest one to the youngest one as A, B, C and D, where A is the oldest alluvium, and consequently, it is the most cohesive and cemented alluvium. The alluvium of Tehran is heterogeneous and strongly cemented, and the cementation between grains is usually the calcite (Fakher et al., 2007). This alluvium often ranges from gravelly sand to sandy gravel with some cobbles and boulders that are dominantly cemented by carbonaceous materials. From a geological point of view, the cementation process of Tehran alluvium is a secondary event, in a way that the cementation agent has been deposited by groundwater after the base grains had been deposited. The cement materials are often carbonate materials such as calcite.

Fig. 3 demonstrates the site on the geological map of Tehran. The classification of alluvium is marked on the map with letters A to D.

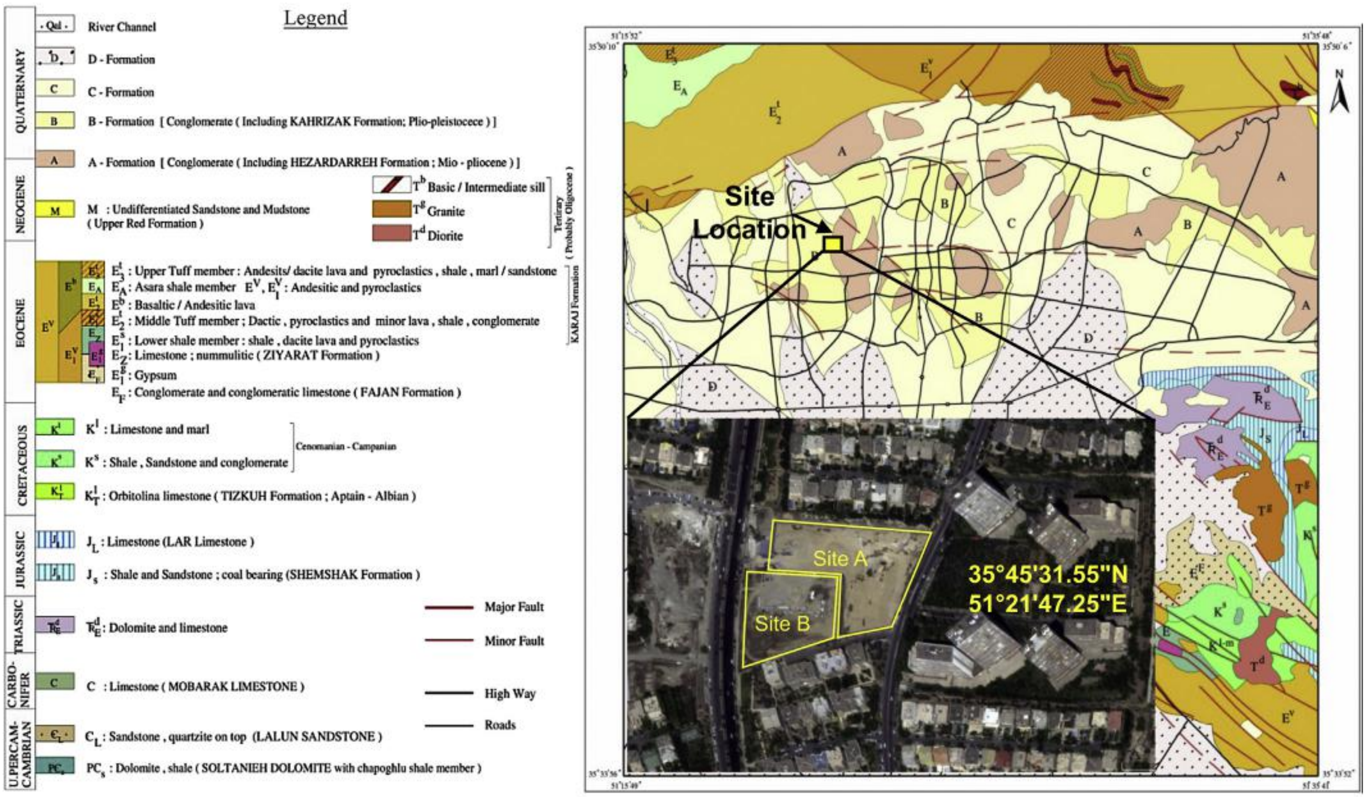

Fig. 3. Classification of Tehran alluvium on the geological map.

Alluviums A and B are in contact at the site. Geological studies indicate that the project site was located almost entirely in type A formation, especially the north wall studied in this paper. Field observation and visual inspection during initial site investigation show evidence of type A alluvium in the northern side of the project site. As illustrated in Fig. 4, it is clear from the texture and color that types A and B are recognized. Type A alluvium tends to dip at an angle of 20° with sandy interlayers as a specific feature, whereas the type B shows grain-size variability and angularity.

In the initial site investigations, 8 boreholes down to 75 m were performed with rotary drilling. The subsoil mainly consisted of sandy and gravely layers with high N_{SPT} (>50), where N_{SPT} is the standard penetration test (SPT) number. It is extremely difficult to acquire undisturbed samples using conventional soil sampling techniques from this material. Furthermore, even when samples can be retrieved, as a block sample, the results of laboratory strength tests may not be representative of the actual in situ behavior. For these reasons, field tests are usually used in conjunction with the conventional index laboratory tests as well as analytical models to estimate in situ cohesion of such alluvial deposits.

Fig. 5 demonstrates the field investigations for studying the in situ properties of coarse-grained cemented alluvium through direct shear and plate load tests. In the initial site investigations, about 100 laboratory direct shear tests were performed on the remolded samples. Due to the fact that the in situ cementation had been removed in remolded samples, these tests cannot represent the in situ cohesion. Soil stiffness parameters were estimated by small strain in situ geophysical (downhole) and medium strain tests (plate load test). Fig. 6a represents the results of laboratory and in situ direct shear tests. In this figure, 4 Coulomb failure envelopes were considered. Failure envelope lines 2 and 4 are for in situ and laboratory tests performed in the initial site investigation phase, respectively, while the envelopes 1 and 3 are for in situ tests carried out after the excavation reaches a depth of 38 m. These tests show the variation in the in situ cohesion of subsoil from the ground surface down to a depth of 35 m. The drained apparent cohesion c' varies between 0 and 83 kPa and the internal friction angle (ϕ') varies between 31° and 41.2°.

4. Original versus revised design

The maximum top elevation of the wall on the north side was +18 m, the bottom elevation in the original design was −20 m, and the excavation reached the elevation of −24.5 m in the final stage. Thus, the maximum excavation depth in the original and revised designs was 38 m and 42.5 m, respectively.

A soil nailing support system was used, and the ultimate limit state and serviceability limit state analyses were performed for design verification.

Stability analysis was performed with SLOPE/W software. A Morgenstern-Price method was implemented to evaluate the safety factor (F_S) against the global instability. Static analysis was performed using the finite element method (FEM), and dynamic (pseudo-dynamic) analyses were only implemented in stability analyses.

FEM was used for calculation of deformation with PLAXIS 2D v8.6, and serviceability limit state control. Geotechnical parameters adopted in the original design using the HS model, with a cautious estimate of the geotechnical parameters, are presented in Table 1. Furthermore, the HS model with small strain stiffness (HSS) was implemented in the revised design. In Table 1, the ranges and average values as well as optimum values (from back analysis) of the soil parameters are represented.

Hardening was assumed isotropic, depending on the plastic shear and volumetric strains. A non-associated flow rule was adopted with respect to frictional hardening and an associated flow rule to the cap hardening. Schanz et al. (1999) and Brinkgreve

Please cite this article as: Alipour A, Eslami A, Design adaptations in a large and deep urban excavation: Case study, Journal of Rock Mechanics and Geotechnical Engineering, https://doi.org/10.1016/j.jrmge.2018.08.014

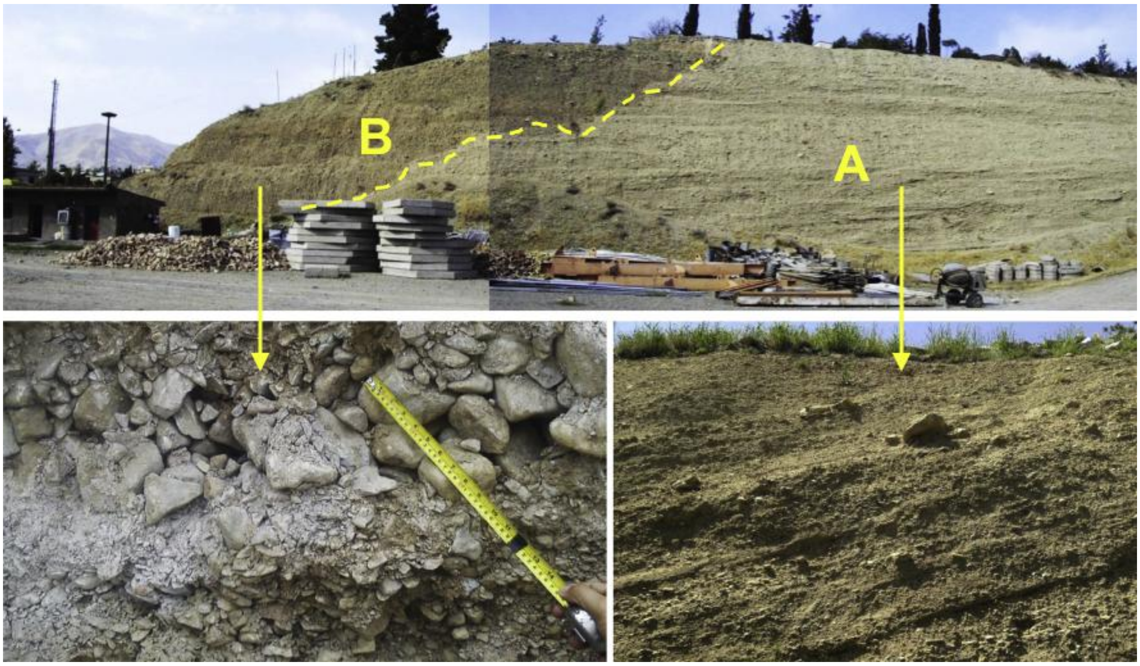

Fig. 4. Visual observations and geological evidences during initial site investigation.

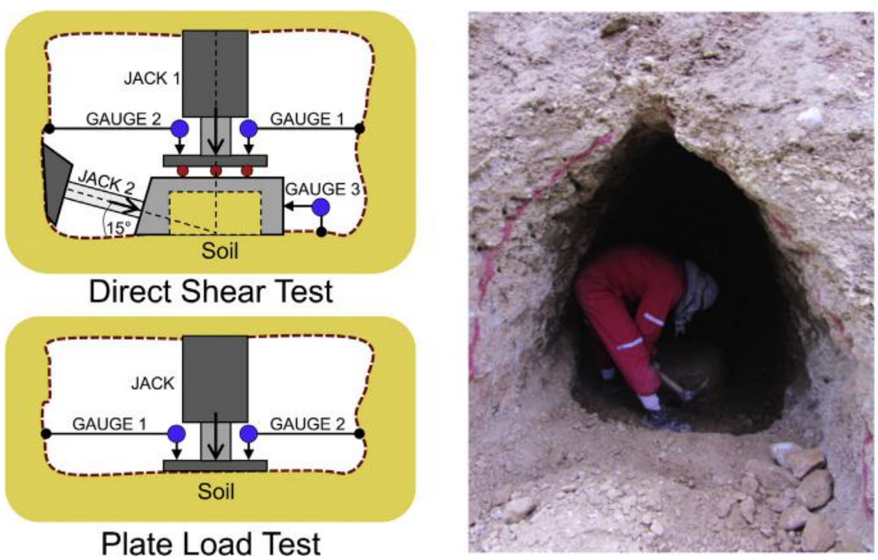

Fig. 5. Preparation for field tests to study the in situ properties of coarse-grained cemented alluvium.

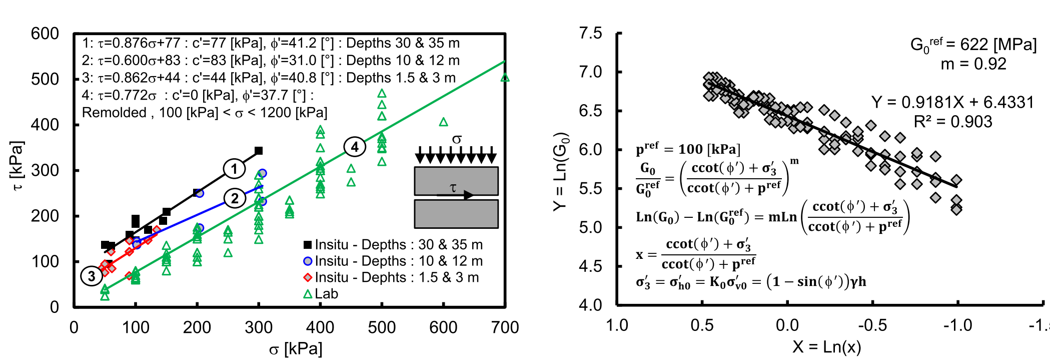

Fig. 6. (a) Results of laboratory and in situ direct shear tests; and (b) determination of *m* and G_0^{ref} from the results of downhole tests.

Table 1
Geotechnical parameters in the original and revised designs.

Design		γ (kN/m^3)	E_{50}^{ref} (MPa)	E_{oed}^{ref} (MPa)	E_{ur}^{ref} (MPa)	G_0^{ref} (MPa)	m	$\gamma_{0.7}$ (10^{-4})	c_{ref} (kPa)	ϕ' (°)	ψ (°)	R_f	ν_{ur}	p^{ref} (kPa)	K_0^{nc}
Original		20	100	100	300	–	0.5	–	50	38	8	0.9	0.2	100	0.38
Revised	Minimum	20	40	40	120	500	0.1	0.8	34	35	5	0.9	0.2	100	0.43
	Maximum	20	180	180	540	750	1	3.5	102	45	15	0.9	0.2	100	0.29
	Average	20	110	110	330	622	0.9	2.15	68	40	10	0.9	0.2	100	0.36
	Optimum	20	110	110	330	622	0.9	0.8	51	40	10	0.9	0.2	100	0.36

Note: E_{50}^{ref} is the secant stiffness from standard drained triaxial test; E_{oed}^{ref} is the tangent stiffness for primary oedometer loading; E_{ur}^{ref} is the unloading/reloading stiffness from drained triaxial test; G_0^{ref} is the reference shear modulus at very small shear strains ($<10^{-6}$); m is the power for stress-level dependency of stiffness; $\gamma_{0.7}$ is the threshold shear strain at which $G_s = 0.722G_0$; c_{ref} is the effective cohesion; ψ is the angle of dilatancy, $\psi = \phi - 30°$, where ϕ is the internal friction angle; R_f is the failure ratio, $R_f = q_f/q_a$; ν_{ur} is the Poisson's ratio for unloading-reloading; p^{ref} is the reference stress; and K_0^{nc} is the K_0-value for normal consolidation, $K_0^{nc} = 1 - \sin\phi'$.

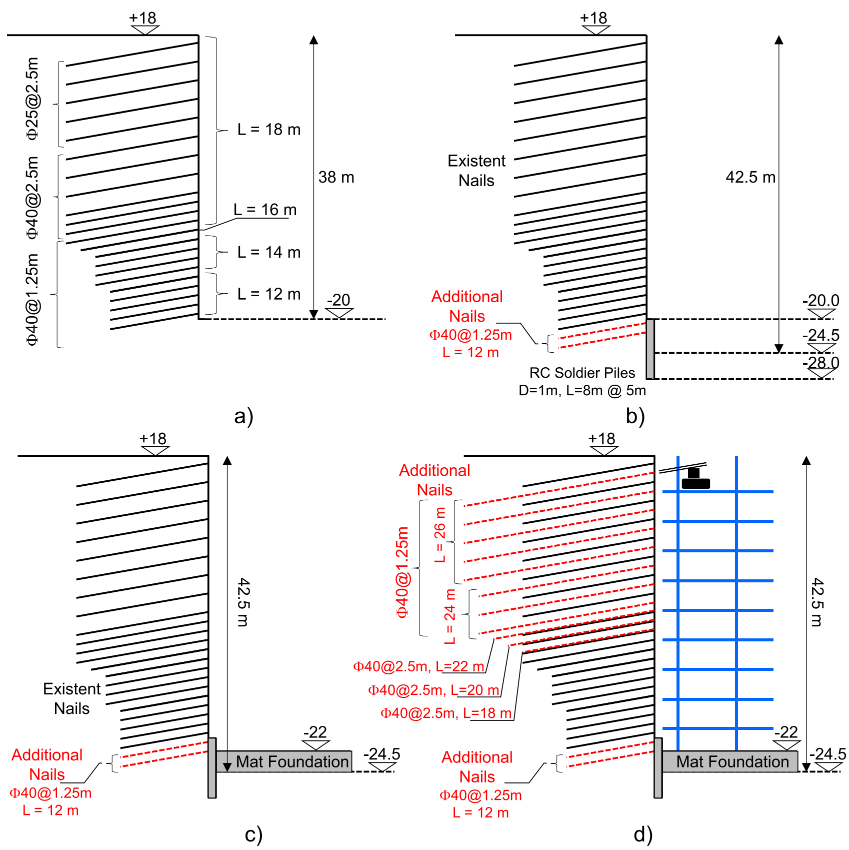

Fig. 7. Construction stages: (a) original design, (b) deepening down to 42.5 m, (c) construction of mat foundation, and (d) construction of main structure together with additional nails. Elevation in m.

(2002) explained in detail the formulation and verification of the HS model. The stress–strain behavior for primary loading is nonlinear. The parameter E_{50} is a confining stress dependent stiffness modulus for primary loading. The amount of stress dependency is controlled by the power m. As illustrated in Fig. 6b, the downhole tests provide the values of G_0^{ref} and m, which are important parameters in the HSS model. Given a power law between the maximum shear modulus of soil (G_0) and in situ confining pressure ($\sigma'_3 = \sigma'_h$), it is easy to calculate m and G_0^{ref} from downhole tests. From regression analysis, m and G_0^{ref} are equal to 0.9 and 622 MPa, respectively.

Solid elements were used to represent the soldier piles in a plane strain analysis. An elastic model with an equivalent elastic modulus E was implemented. The elastic modulus of concrete was 30 GPa, the pile diameter was 1 m, and the pile spacing was 5 m. These resulted in an equivalent elastic modulus of 4.7 GPa. The Poisson's ratio was assumed as 0.2 for the solid element.

Nails were modeled in PLAXIS using geogrid elements. A class AIII steel material with yield tensile strength of 400 MPa and elastic modulus of 200 GPa was used. The shotcrete facing was modeled using the elastic plate elements with the thickness of 100 mm, axial stiffness (EA) of 2.1×10^6 kN/m, and flexural stiffness (EI) of 1750 kN m^2/m.

Fig. 7 presents the construction history in four stages. First, based on the original design, excavation was performed down to an elevation of −20 m. In stage 2, based on the revised soil parameters and extra site investigations, two extra rows of nails were implemented in combination with cast-in-place concrete soldier piles, 8 m in length, 1 m in diameter, and 5 m in spacing, at the bottom of the wall. The excavation in this stage was performed down to an elevation of −24.5 m (equivalent to a depth of 42.5 m). In the following phase, the concrete soldier piles were connected to the main building mat foundation to create a lateral support at the bottom of the retaining system. All of the phases up to this stage were temporary works and the durability concerns and seismic effects came into consideration afterward. In the final phase, additional nails were performed in parallel to the construction of the main building. These additional galvanized nails accounted for corrosion protection and permanent situations. Fig. 8 illustrates the calculation for the lateral support effect of mat foundation. The main building would produce a normal (gravitational) force, which is calculated as follows:

$$N = B\left(nw + t_f\gamma_c\right) \tag{3}$$

where N is the normal force per unit length; n is the number of total floors, $n = 31$; w is the dead load for each floor, $w = 6$ kPa; t_f is the thickness of the foundation, $t_f = 2.5$ m; and γ_c is the unit weight of concrete, $\gamma_c = 24$ kN/m^3. The foundation lateral resistance produced by the vertical force N in the ultimate state is calculated as

$$T = N\tan\delta \tag{4}$$

where δ is the friction angle between the concrete and soil, and $\delta = \phi'/3$ ($\sim$13.3°) in this study). A total ultimate resistance of approximately 3000 kN/m was mobilized when the north wall moved toward the building. This frictional resistance was implemented in the ultimate limit state analysis to account for the long-term performance of the retaining system in pseudo-dynamic stability analysis. It was assumed that T would be activated as a lateral support during the earthquake and consequently, in combination with the soldier piles, would prevent the soil below the elevation of +20 m from moving. The top elevation of the soldier piles is +20 m, same as the bottom elevation of excavation in the original design.

Table 2 lists the global safety factors calculated by limit equilibrium analyses. Each value represents a "design situation". According to Lazarte et al. (2003), for the soil nailing retaining system in the long-term condition, a minimum global safety factor of 1.35 is adequate for temporary and 1.5 for permanent structures. For a short-term condition during temporary excavation works, a minimum safety factor of 1.2–1.3 is recommended. For seismic analyses (pseudo-dynamic), a minimum safety factor of 1.1 for temporary and permanent structures in long term is recommended. The dimensionless lateral seismic coefficient k_h used in pseudo-dynamic analyses could be calculated conservatively as follows (Lazarte et al., 2003):

$$k_h = 0.67A(A - 1.45) \tag{5}$$

where A represents the PGA. The PGA in Tehran is given as 0.35 g according to the Iranian seismic code (BHRC, 2007). Thus, a value of 0.2 is calculated for the dimensionless lateral seismic coefficient k_h.

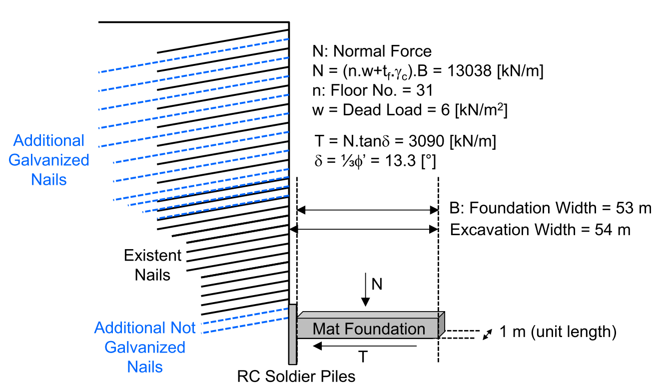

Fig. 8. Lateral support at the bottom of the wall produced by the building foundation.

Table 2
Global safety factors in allowable stress design (ASD) approach.

No.	Description	Height of ramp, h_e (m)	F_S
a	Static stability analysis with initial geotechnical parameters	38	1.303
b	Static stability analysis with revised geotechnical parameters	38	1.493
c	Static stability analysis with revised geotechnical parameters	42.5	1.341
d	Static stability analysis with revised geotechnical parameters, 30% reduction in cross-section of existing rebar	42.5	1.611
e	Pseudo-dynamic stability analysis with revised geotechnical parameters, $k_h = 0.2$, 30% reduction in cross-section of existing rebar	42.5	1.187

In order to consider the long-term performance of steel rebars, it is necessary to galvanize additional nails. For existing rebar, solutions such as extensive protection or reduction in the available cross-section due to the subsequent corrosion could be implemented. The reduction in the existing rebar cross-section was implemented in this project. This variant was not needed for future maintenance measures and related costs. According to OCDI (2009), the corrosion rate of steel (in mm/a) could be calculated with regard to the environmental conditions. Soil and water chemical and electrical resistivity tests showed a moderate corrosion potential in this project. The nails are embedded in the soil and exposed to water flows occasionally. As a result, the following two situations in the landside were considered according to Table 3 (after OCDI, 2009):

(i) above the ground surface and exposed to air: with the corrosion rate of 0.1 mm/a; and
(ii) underground (above the residual water level): with the corrosion rate of 0.03 mm/a.

An average of these two extreme values was considered as the corrosion rate of rebar in this project (i.e. 0.065 mm/a). At this rate, after 50 years (design life), a reduction in diameter (6.5 mm) is estimated. For ϕ40 nails, this leads to 30% reduction in the cross-section, and for ϕ25 nails, the reduction is about 50%. These values are used for calculations of the safety factor in the final stage.

5. Observations and inverse analysis

Due to the fact that excavation had been stable during the long period of construction, an observational approach was implemented to re-investigate the geotechnical parameters of this long-standing existing retaining system from complementary site investigations, additional in situ tests, observations, and monitoring data.

During excavation, an access ramp was planned for temporary construction works. The stability analysis was implemented to estimate the mobilized average effective in situ cohesion (c'_{ave}). Fig. 9 presents the relationship between the height of ramp (h_e) and the average effective in situ cohesion (c'_{ave}) mobilized for the stability of

Table 3
Recommended values for corrosion rate in the landside according to OCDI (2009).

Corrosive environment		Corrosion rate (mm/a)
Landside	Above the ground and exposed to air	0.1
	Underground (above the residual water level)	0.03
	Underground (bellow the residual water level)	0.02

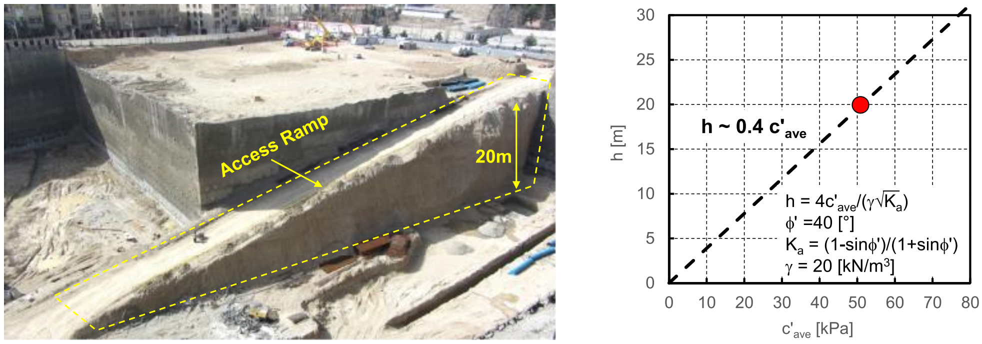

Fig. 9. Stability back analysis of access to calculate c'_{ave}.

the wall. In the calculations, soil unit weight and internal friction angle were given as 20 kN/m^3 and 40°, respectively. A minimum value close to 50 kPa for c'_{ave} was calculated considering $h_{\mathrm{e}} = 20$ m. This mobilized average effective in situ cohesion is in accordance with those obtained from in situ direct shear tests presented previously.

Because the range of monitored deformation was small, high stiffness ranges mobilized in the initial stages of excavation should be considered in the modeling. Fig. 10 depicts the geotechnical parameters measured from field investigations, including the maximum shear modulus (G_0) from downhole tests performed in 4 boreholes, elastic modulus in unloading and reloading (E_{ur}), elastic modulus in primary loading (E_{50}) from plate load test, and c' from the direct shear test. In addition, the geometry of the finite element model is illustrated.

To determine the most important and effective soil model parameters that influence the deformation behavior of the retaining wall, sensitivity analysis was performed. The sensitivity was calculated according to a simple method given by EPA (1999). In this method, three major coefficients, namely the sensitivity ratio (Eq. (6)), sensitivity score (Eq. (7)), and relative sensitivity (Eq. (8)) for each input variable ($x_{\mathrm{L,R}}$) with respect to any system response were calculated. The sensitivity ratio (η_{SR}) is defined as the percentage change in the output divided by the percentage change in the input for a specific input variable. The ratio of the total range over a reference value, x, is used for weighing, which makes the sensitivity ratio independent of the unit of the variable. The sensitivity score (η_{SS}) of each input variable to a system response A (e.g. displacement) at all construction steps can be simply added up to be representative η_{SS,A_i} for the whole construction sequence. Then the relative sensitivity of the system response A is obtained by Eq. (8):

$$\eta_{\mathrm{SR}} = \frac{\left[f(x_{\mathrm{L,R}}) - f(x)\right]/f(x)}{(x_{\mathrm{L,R}} - x)/x} \tag{6}$$

$$\eta_{\mathrm{SS}} = \eta_{\mathrm{SR}} \frac{x_{\mathrm{R}}^{\max} - x_{\mathrm{R}}^{\min}}{x} \tag{7}$$

$$\alpha_A(x_i) = \frac{\eta_{\mathrm{SS},A_i}}{\sum\limits_{i=1}^{N} \eta_{\mathrm{SS},A_i}} \tag{8}$$

Finally, the total relative sensitivity, $\alpha(x_i)$, for each input variable is given by the following equation:

$$\alpha(x_i) = \frac{\eta_{\mathrm{SS},i}}{\sum\limits_{i=1}^{M} \eta_{\mathrm{SS},i}} \tag{9}$$

where M is the number of system responses.

Fig. 11 shows the geodesic targets attached to the north wall for deformation monitoring. T-targets were attached first and then N-

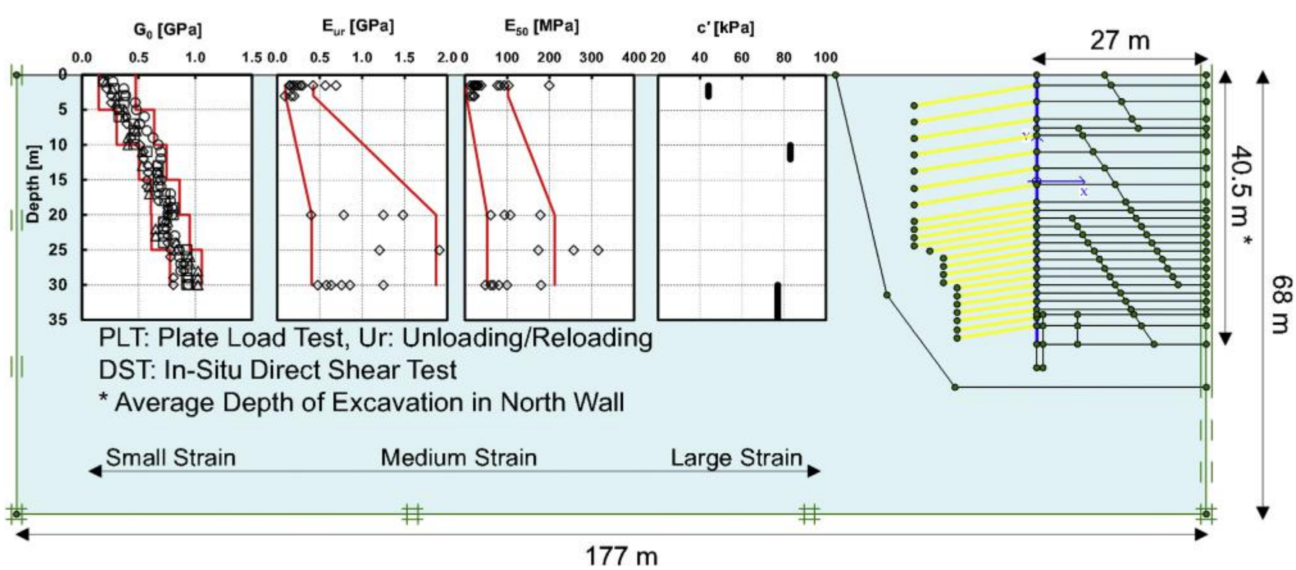

Fig. 10. Geometry of numerical model together with subsoil geotechnical parameters.

Please cite this article as: Alipour A, Eslami A, Design adaptations in a large and deep urban excavation: Case study, Journal of Rock Mechanics and Geotechnical Engineering, https://doi.org/10.1016/j.jrmge.2018.08.014

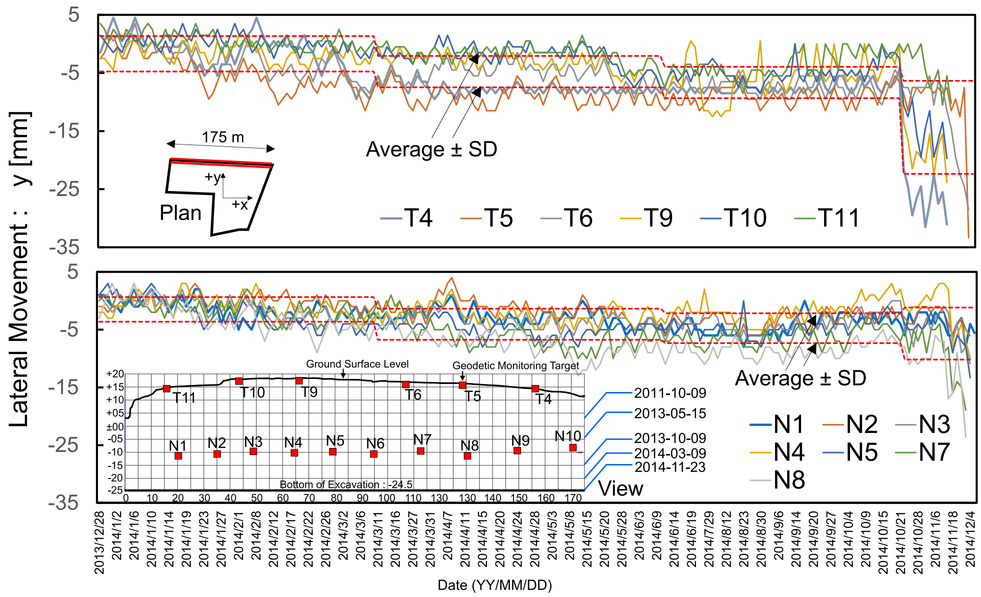

Fig. 11. Geodesic monitoring of lateral wall movements of north wall during excavation and after revised design in target series T and N.

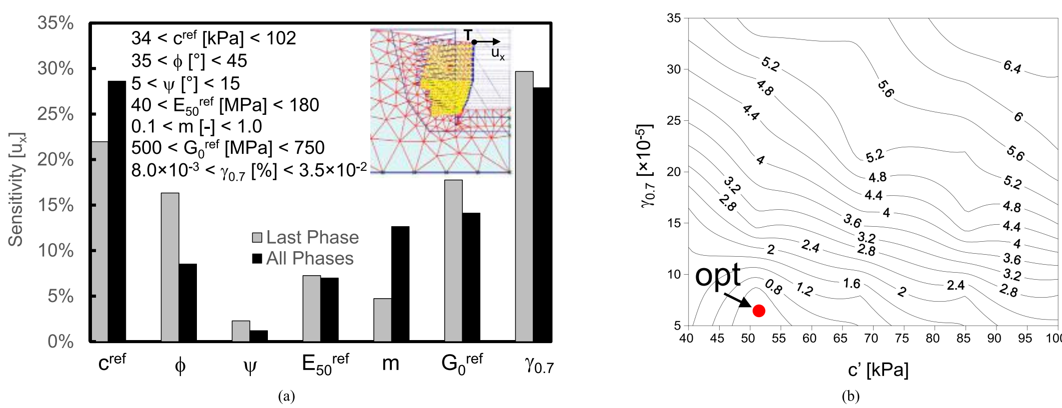

Fig. 12. (a) Effective parameters in sensitivity analysis and (b) optimum solution to minimize error function.

targets were attached after the excavation reached the elevation of −15 m. In addition, Fig. 11 also presents the results of lateral movements of the north wall during excavation. The results are scattered but there is a general trend that shows an increase in horizontal movements with the deepening of excavation. Due to the lack of information, only the results in the final stage of excavation existed. The construction sequences were modeled according to available pictures taken during the project and topographic drawn from geodesic surveying. In addition, standard deviations (SDs) of input parameters and monitoring data were considered to estimate the range of the variation.

Fig. 12a shows the total sensitivity of horizontal movement of point T with respect to the soil model parameters c_{ref}, ϕ, E_{50}^{ref}, m, G_0^{ref} and $\gamma_{0.7}$. The most important parameters, in this case, are c_{ref} and

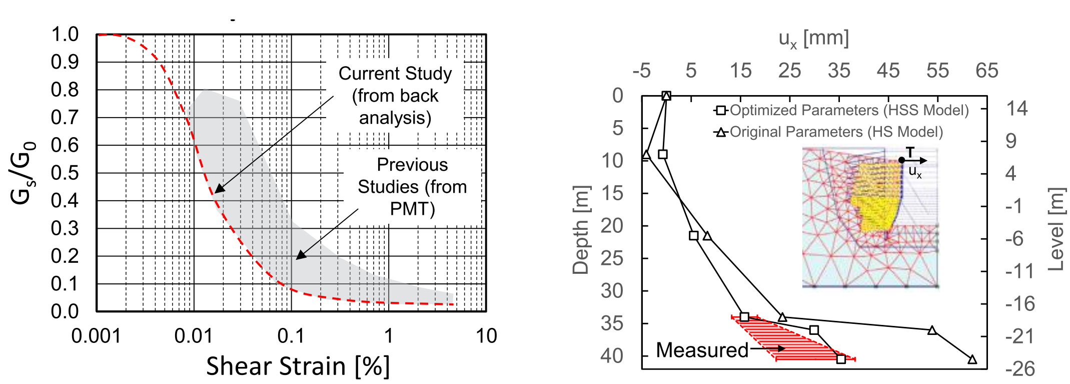

Fig. 13. (a) Normalized secant shear stiffness reduction curve for type A Tehran alluvium (Sangtarashha et al., 2011) and (b) calculated and measured lateral deformations.

Please cite this article as: Alipour A, Eslami A, Design adaptations in a large and deep urban excavation: Case study, Journal of Rock Mechanics and Geotechnical Engineering, https://doi.org/10.1016/j.jrmge.2018.08.014

$\gamma_{0.7}$, which affect the maximum horizontal deformation of the wall. Therefore, the optimum values for these parameters to minimize the absolute difference between measured and calculated lateral wall movements (the error function) were estimated by back analysis. Fig. 12b illustrates the contours of error function to estimate the optimum values.

These optimum values are comparable with previous studies in Tehran alluvium. According to the back-calculated $\gamma_{0.7}$ equal to 0.8×10^{-4}, a reduction curve can be estimated and is depicted in Fig. 13a. This curve is in the lower limit of those obtained from pressuremeter test (PMT) results, as reported for type A Tehran alluvium (Sangtarashha et al., 2011). In addition, the average effective cohesion c'_{ave} back-calculated from deformation monitoring data is in accordance with those obtained from previous stability back analysis and in situ direct shear tests.

Fig. 13b presents a prediction of horizontal deformation from original (HS) and revised (HSS) models (Finno et al., 2002, 2007; Benz, 2007) in comparison with the measured data. The trend of monitoring data is compatible with that of the revised model. Due to the lack of monitoring data from the beginning of the project, results were set from the beginning of revised prediction where the depth of excavation was about 34 m. With consideration of measurement error form the SD of monitoring data, it was found that the measurements are compatible with the revised model prediction. Thus, it could be concluded that the deformations are relatively in the lower limit of prediction.

As stated earlier, local water resources such as sewers, pipe leakages, and groundwater flow due to irrigation and precipitation usually are the main causes for implementing a draining system in excavation works. The excavation was performed in the nearly dry condition. The local groundwater and underground streams regularly were pumped out of the site during excavation. Weep-hole drains were introduced to transfer the local water behind the wall.

6. Conclusions

In the northwest of Tehran, a deep and large nailed excavation with a maximum height of 38 m had been constructed during about 2 years. An over-digging from 38 m to 42.5 m was determined. The project was large in the plan as well as in the depth. Furthermore, due to a nearby excavation, an unbalanced force was imposed to the project main building in the future. Thus, another issue was upgrading the temporarily existent retaining system to the permanent one.

The subsoil consisted of cemented coarse-grained formation with high stiffness and strength properties. This alluvium was very heterogeneous, consisting of cobbles and boulders. Thus, in situ full-scale tests must be considered as appropriate alternatives to estimate ground properties. The findings of in situ tests showed that the apparent cohesion in the project site ranges from about 40 kPa to 80 kPa. Thus, the exact values must be determined from back analysis of the actual performance of the system. In the same manner, the stiffness parameters are in a wide range that imposes difficulties in selecting appropriate design values.

With an observational approach, it is shown that the implementation of HSS model with consideration of small stiffness parameters from downhole and back analysis data has improved the performance prediction of the retaining system in comparison with the deformation monitoring data. Thus, the modification of the model and the parameters could remarkably have amended the design.

By adapting the existent support system through additional nails as well as the implementation of soldier piles, it is concluded that the deepening of the excavation down to 42.5 m can be feasible. It was found that building mat foundation provides remarkable high lateral frictional resistance that could be implemented as a lateral support at the bottom part of the excavation wall.

Implementation of the galvanized new nails and the reduction in the cross-section of the old nails are a practical variant to deal with such situations to upgrade durability and long-term stability of existing retaining system.

Conflicts of interest

The authors wish to confirm that there are no known conflicts of interest associated with this publication and there has been no significant financial support for this work that could have influenced its outcome.

References

Arai K, Ohta H, Kojima K. Estimation of soil parameters based on monitored movement of subsoil under consolidation. Soils and Foundations 1984;24(4):95–108.
Arai K, Ohta H, Kojima, Wakasugi M. Application of back-analysis to several test embankments on soft clay deposits. Soils and Foundations 1986;26(2):60–72.
Benz T. Small strain stiffness of soils and its numerical consequences [PhD Thesis]. Stuttgart, Germany: University of Stuttgart; 2007.
Brinkgreve RBJ. PLAXIS finite element code for soil and rock analysis. version 8. Rotterdam: A.A. Balkema; 2002.
Building and Housing Research Center (BHRC). Iranian code of practice for seismic resistant design of building [standard 2800 – 3rd edition]. Tehran, Iran: BHRC; 2007.
Calvello M. From the observational method to "observational modelling" of geotechnical engineering boundary value problems. In: Huang J, Fenton GA, Zhang L, Griffiths DV, editors. Geo-risk 2017: geotechnical risk assessment and management. American Society of Civil Engineers (ASCE); 2017. p. 101–17. https://doi.org/10.1061/9780784480731.008.
Chapman T, Green G. Observational method looks set to cut city building costs. Proceedings of the Institution of Civil Engineers – Civil Engineering 2004;157(3):125–33.
Durgunoglu HT, Keskin HB, Kulac HF, Ikiz S, Karadaylar T. Performance of very deep temporary soil nailed walls in Istanbul. In: Earth reinforcement in cut, XIV ISSMGE, Madrid, Spain; 2007. p. 559–64.
Durgunoglu HT. Performance of deep soil nailed walls. In: The 6th international conference on case histories in geotechnical, Arlington, USA; 2008. Paper No. JKM 5.
Fakher A, Cheshomi A, Khamechiyan M. The addition of geotechnical properties to a geological classification of coarse-grained alluvium in a pediment zone. Quarterly Journal of Engineering Geology and Hydrogeology 2007;40:163–74.
Finno RJ, Blackburn JT, Roboski JF. Three-dimensional effects for supported excavations in clay. Journal of Geotechnical and Geoenvironmental Engineering 2007;133(1):30–6.
Finno RJ, Bryson S, Calvello M. Performance of a stiff support system in soft clay. Journal of Geotechnical and Geoenvironmental Engineering 2002;128(8):660–71.
Finno RJ, Calvello M. Supported excavations: observational method and inverse modeling. Journal of Geotechnical and Geoenvironmental Engineering 2005;131(7):826–36.
Fuentes R, Pillai A, Ferreira P. Lessons learnt from a deep excavation for future application using the observational method. Journal of Rock Mechanics and Geotechnical Engineering 2018;10(3):468–85.
Gastebled OJ, Baghery S. 3D modelling of a deep excavation in a sloping site for the assessment of induced ground movements. In: Benz T, Nordal S, editors. Numerical methods in geotechnical engineering. London: Taylor & Francis Group; 2010.
Gens A, Ledesma A, Alonso EE. Back analysis using prior information – application to the staged excavation of a cavern in rock. In: Swoboda G, editor. Numerical methods in geomechanics, proceedings of the 6th international conference on numerical methods in geomechanics. Rotterdam, the Netherlands: A.A. Balkema; 1988. p. 2009–16.
Gens A, Ledesma A, Alonso EE. Estimation of parameters in geotechnical back-analysis – II. Application to a tunnel excavation problem. Computers and Geotechnics 1996;18(1):29–46.
Gioda G, Maier G. Direct search solution of an inverse problem in elastoplasticity: identification of cohesion, friction angle and in situ stress by pressure tunnel tests. International Journal for Numerical Methods in Engineering 1980;15(2):1823–48.
Gioda G. Indirect identification of the average elastic characteristics of rock masses. In: Pells PJN, editor. Structural foundations on rock: proceedings of the international conference on structural foundations on rock, vol. 1. A.A. Balkema; 1980. p. 65–73.

Please cite this article as: Alipour A, Eslami A, Design adaptations in a large and deep urban excavation: Case study, Journal of Rock Mechanics and Geotechnical Engineering, https://doi.org/10.1016/j.jrmge.2018.08.014

Glass PR, Powderham AJ. Application of the observational method at the limehouse link. Géotechnique 1994;44(4):665–79.
Hisatake M, Ito T. Back analysis for tunnels by optimization method. In: Kawamoto T, Itikawa Y, editors. Numerical methods in geomechanics, Nagoya 1985: proceedings of the 5th international conference on numerical methods in geomechanics. A.A. Balkema; 1985. p. 1301–7.
Ikuta Y, Maruoka M, Aoki M, Sato E. Application of the observational method to a deep basement excavated using the top-down method. Géotechnique 1994;44(4):655–79.
Lazarte CA, Elias V, Espinoza RD, Sabatini PJ. Geotechnical engineering circular no. 7 – soil nail walls (Report no. FHWA0-IF-03-017). Washington, D.C., USA: Federal Highway Administration, US Department of Transportation; 2003.
Ledesma A, Gens A, Alonso EE. Estimation of parameters in geotechnical back-analysis – I. Maximum likelihood approach. Computers and Geotechnics 1996;18(1):1–27.
Ledesma A, Romero E. Systematic back analysis in tunnel excavation problems as a monitoring technique. In: Proceedings of the 14th international conference on soil mechanical and foundations engineering, vol. 3. A.A. Balkema; 1997. p. 1425–8.
Ledesma A. Identification de parametros en geotecnia. Aplicacibn a la excavacion de tt'meles [PhD Thesis]. Barcelona, Spain: Technical University of Catalunya; 1987 (in Spanish).
Peck RB. Advantages and limitations of the observational method in applied soil mechanics. Géotechnique 1969;19(2):171–87.
Peck RB. The observational method can be simple. Proceedings of the Institution of Civil Engineers – Geotechnical Engineering 2001;149(2):71–4.
Pinto A, Pereira A, Villar M. Deep excavation for the new central library of Lisbon. In: Proceedings of the 14th European conference on soil mechanics and geotechnical engineering, Madrid, Spain, vol. 2; 2007. p. 623–8.
Powderham AJ, Rutty P. The observational method in value engineering. In: Proceedings of the 5th international conference and exhibition on piling and deep foundations, Bruges, Belgium. Deep Foundations Institute; 1994.
Powderham AJ. An overview of the observational method: development in cut and cover and bored tunnelling projects. Géotechnique 1994;44(4):619–36.
Powderham AJ. The observational method – learning from projects. Proceedings of the Institution of Civil Engineers – Geotechnical Engineering 2002;115(1):59–69.
Rieben EH. Geological observations on alluvial deposits in northern Iran. Geological Survey of Iran; 1966.
Sakurai S, Akutagawa S, Takeuchi K, Shinji M, Shimizu N. Back analysis for tunnel engineering as a modern observational method. Tunnelling and Underground Space Technology 2003;18(2–3):185–96.
Sakurai S, Takeuchi K. Back analysis of measured displacement of tunnel. Rock Mechanics and Rock Engineering 1983;16(3):173–80.
Sakurai S. Displacement measurements associated with the design of underground openings. In: Kovari AA, editor. Proceedings of the international symposium on field measurements in geomechanics, vol. 2. Rotterdam, the Netherlands: A.A. Balkema; 1983. p. 1163–78.
Sangtarashha K, Fakher A, Pahlevan B. Variation of stiffness of Tehran coarse-grained soil with depth and strain. In: Chung CK, Kim HK, Lee JS, Jung YH, Kim DS, editors. Deformation characteristics of geomaterials: proceedings of the 5th international symposium on deformation characteristics of geo-materials (IS-Seoul 2011). IOS Press; 2011. p. 1007–18.
Schanz T, Vermeer PA, Bonnier PG. The hardening soil model: formulation and verification. In: Beyond 2000 in computational geotechnics – 10 years of PLAXIS. Rotterdam: A.A. Balkema; 1999.
Spross J, Johansson F. When is the observational method in geotechnical engineering favorable? Structural Safety 2017;66:17–26.
Tan Y, Wang DL. Characteristics of a large-scale deep foundation pit excavated by the central-island technique in Shanghai soft clay. I: bottom-up construction of the central cylindrical shaft. Journal of Geotechnical and Geoenvironmental Engineering 2013;139(11):1875–93.
Terzaghi K, Peck RB. Soil mechanics engineering practice. John Wiley; 1948.
The Overseas Coastal Area Development Institute of Japan (OCDI). Technical standards and commentaries for port and harbor facilities in Japan. OCDI; 2009.
US Environmental Protection Agency (EPA). Total risk integrated methodology (TRIM): TRIM. FaTE technical support document. In: Description of module, vol. I. EPA; 1999. EPA-453/D-99-002A.
Yeow H, Feltham I. Case histories back analyses for the application of the observational method under Eurocodes for the Scout project. In: The 6th international conference on case histories in geotechnical engineering. Arlington, USA: Missouri University of Science and Technology; 2008. p. 1–13.
Yeow HC, Nicholson D, Man CL, Ringer A, Glass P, Black M. Application of observational method at crossrail Tottenham Court Road station, UK. Proceedings of the Institution of Civil Engineers – Geotechnical Engineering 2014;167(2):182–93.
Young DK, Ho EWL. The observational approach to design of a sheet-piled retaining wall. Géotechnique 1994;44(4):637–54.
Zhang WG, Goh ATC, Zhang YM. Updating soil parameters using spreadsheet method for predicting wall deflections in braced excavations. Geotechnical and Geological Engineering 2015;33(6):1489–98.
Zhang WG, Zhang RH, Goh ATC. Multivariate adaptive regression splines approach to estimate lateral wall deflection profiles caused by braced excavations in clays. Geotechnical and Geological Engineering 2018;36(2):1349–63.
Zhang WG, Zhang YM, Goh ATC. Multivariate adaptive regression splines for inverse analysis of soil and wall properties in braced excavation. Tunnelling and Underground Space Technology 2017;64:24–33.

Amir Alipour received his BSc degree in Civil Engineering from University of Guilan, Iran, in 2006, MSc degree in Geotechnical Engineering from Ferdowsi University of Mashhad (FUM), Iran, in 2011, respectively, and he is a PhD candidate in Geotechnical Engineering at Amirkabir University of Technology (AUT), Iran. He is also a professional geotechnical engineer with 10-year experience as designer and supervisor in a wide range of projects including site investigation, earth retention system, underground excavation, foundation, ground improvement, performance monitoring, and instrumentation. He has a strong background in three-dimensional (3D) numerical modeling, sensitivity, reliability, and inverse analyses, interpretation, identification, and correction of systematic errors in monitoring data, macro programming to automate procedures in windows, and development of risk management plan with the observational method (OM).

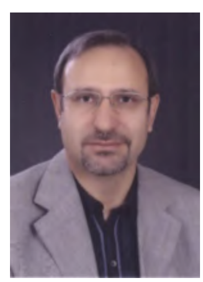

Abolfazl Eslami received his BSc and MSc degrees in Structural and Geotechnical Engineering from Sharif University of Technology (SUT) and Amirkabir University of Technology (AUT), Iran, in 1985 and 1988, respectively. He has acquired PhD degree in Geotechnical Engineering from the University of Ottawa, Canada, in 1997. He is a Professor in Geotechnical Engineering at AUT in Civil Engineering Department. With cooperation of Prof. B.H. Fellenius, E & F Method (UniCone Program) has been developed for soil identification and pile design using cone penetration test (CPT) and piezocone penetration test (CPTu) records during 1997–2002. Also, he has served as an Associate Professor in Department of Civil Engineering at University of Guilan from 1997 to 2006. His research interests are mainly in deep and special foundations, in situ testing in geotechnical practice, ground modification and geo-systems. He has published more than 70 ISI journal papers, 25 national journal papers, 50 international conference papers, 30 national conference papers and 7 text books and handbooks in foundation and geotechnical engineering. He has consulted, participated and practiced in a large number of specific substructure projects.

Please cite this article as: Alipour A, Eslami A, Design adaptations in a large and deep urban excavation: Case study, Journal of Rock Mechanics and Geotechnical Engineering, https://doi.org/10.1016/j.jrmge.2018.08.014